EasyChair Preprint

№ 11949

Controllable Deep Learning Denoising Model for Ultrasound Images Using Synthetic Noisy Image

Mingfu Jiang, Chenzhi You, Mingwei Wang, Heye Zhang, Zhifan Gao, Dawei Wu and Tao Tan

February 5, 2024

Controllable Deep Learning Denoising Model for Ultrasound Images Using Synthetic Noisy Image

Mingfu Jiang[1,5#], Chenzhi You[2#], Mingwei Wang[3], Heye Zhang[4], Zhifan Gao[4], Dawei Wu[2*], and Tao Tan[1*]

[1] Faculty of Applied Sciences, Macao Polytechnic University, Macao 999078, China
[2] State Key Laboratory of Mechanics and Control for Aerospace Structures, Nanjing University of Aeronautics and Astronautics, Nanjing 210016, China.
[3] Department of Dardiovascular Medicine, Affiliated Hospital of Hangzhou Normal University, Hangzhou 311121, China
[4] School of Biomedical Engineering, Sun Yat-sen University, Shenzhen 518107, China
[5] College of Information Engineering, Xinyang Agriculture and Forestry University, Xinyang 464000, China

[#]Mingfu Jiang and Chenzhi You contribute equally
*Corresponding author: Tao Tan (taotan@mpu.edu.mo) and Dawei Wu (dwu@nuaa.edu.cn)

Abstract. Medical ultrasound imaging has gained widespread prevalence in human muscle and internal organ diagnosis. Nevertheless, various factors such as the interference effect of ultrasonic echoes, mutual interference between scattered beams, inhomogeneity and uncertainty in the spatial distribution of human body tissue, inappropriate operation, and imaging signal transmission processes, can lead to noise and distortion in ultrasound images. These factors make it difficult to obtain clean and accurate ultrasound images, which may adversely affect medical diagnosis and treatment processes. While traditional denoising methods are time-consuming, they are also not effective in removing speckle noise while retaining image details, leading to potential misdiagnosis. Therefore, there is a significant need to accurately and quickly denoise medical ultrasound images to enhance image quality. In this paper, we propose a flexible and lightweight deep learning denoising method for ultrasound images. Initially, we utilize a considerable number of natural images to train the convolutional neural network for acquiring a pre-trained denoising model. Next, we employ the plane-wave imaging technique to generate simulated noisy ultrasound images for further transfer learning of the pre-trained model. As a result, we obtain a non-blind, lightweight, fast, and accurate denoiser. Experimental results demonstrate the superiority of our proposed method in terms of denoising speed, flexibility, and effectiveness compared to conventional convolutional neural network denoisers for ultrasound images.

Keywords: Plane-wave Imaging, Noise Transfer Learning, Non-blind Ultrasound Image Denoising, Lightweight Model.

1 Introduction

Ultrasound imaging has become a widely used medical imaging modality due to its relative safety, affordability, and portability [1]. Unfortunately, hardware acquisition and ultrasound scattering can introduce severe noise into the signal, leading to corrupt textural structure and image details and impeding the clinician's accurate diagnosis and assessment. The difficulty of reducing the above-mentioned noise arises due to its tissue-dependent and non-uniform modeling. The generation of noise in medical ultrasound images is a complex phenomenon, attributable to the interaction of backscattered coherent waves from multiple fundamental scatterers with varying phases, resulting in random and constructive or destructive disturbances. This interference is labeled as speckle noise, a granular texture pattern that may potentially provide useful diagnostic information [2]. Speckle noise affects all coherent imaging systems, including medical ultrasound [3], and exhibits multiplicative behavior that is strongly associated with non-Gaussian statistics. Conventional filtering techniques are not suitable for addressing speckle noise due to their primary design to suppress additive noise. Although several advanced processing methods have been developed by researchers to eliminate or reduce speckle noise, they do not consider preserving important details such as edges and lines in the image [4][5]. Consequently, eliminating speckle noise from medical ultra-sound images while preserving pertinent details remains a "classical challenge" for researchers.

Most current deep learning-based ultrasound denoising methods are constrained by the scarcity of training images and clean images. G. Sobhan, et al. [6] proposed a novel beamforming method based on deep learning that accurately maps pre-beamformed channel data to the output image by leveraging a sufficient number of ground-truth echogenicity maps obtained from the transformation of real photographic images. Their method successfully improved resolution and contrast of plane-wave imaging while preserving frame rate, addressed the scarceness of training and labeled data, and removed background speckle noise in ultrasound images. Nonetheless, their model did not employ the Dirac delta function as the point-spread function (PSF) for ultrasound image formation, thus only reducing background speckle noise without considering other interfering clutter embedded in the actual ultrasound images such as side lobes and grating lobes. All the existing learning methods have the challenge of obtain the ground truth of clean ultrasound image.

In stead of working on the imaging end, this paper presents a deep learning-based denoising model for ultrasound images as a post-processing step. We utilize synthetic noisy images to achieve precise control. The proposed approach is capable of efficiently eliminating various noises such as speckle noise, while preserving image details. Code is available at: https://github.com/daming876/image-denoise.

2 Related Work

2.1 Deep Learning Network Denoiser

The denoising methods can be divided into three categories: filter-based, model-based, and machine learning and deep learning algorithm. Dabov, Kostadin et al. proposed BM3D [7], which utilizes sparse representation in the transform domain, non-local image similarity, and a 3D filtering method based on block matching to achieve strong image denoising performance, and small mean squared error. Gu [8] used different weighting characteristics of the WNNM algorithm and image non-local self-similarity to obtain better model-based image denoising results. However, these traditional methods are difficult to deal with the non-smooth part of the image, and the texture information of the image can not be effectively preserved while denoising, generally the image is blurred after denoising. With the development of deep learning technology, many researchers put forward the method of using deep learning to denoise images. Sil, et al. [9] proposed a method that utilizes convolutional neural network transfer learning for image classification and denoising. This method can accurately predict the noise model and is particularly effective for blind image denoising. Zhang et al. [10] introduced a method which is Residual Learning of Deep CNN for Image Denoising (DnCNN), which employs the residual algorithm for gradual improvement of CNN models. However, these methods tend to be limited in their effectiveness for specific noise levels, thus restricting their versatility. As a solution, Zhang Kai et al. developed an fast and flexible denoising network (FFDNet) [11] for denoising, based on DnCNN. The FFDNet method downsamples the input image and divides it into four sub-images, each sub-image acquiring an eigenvalue, followed by the addition of noise generated through the Additive White Gaussian Noise (AWGN) method. After CNN processing, upsampling is performed to regain the overall output image. The resulting image is denoised through the successful FFDNet method, which manifests improved denoising effects on images with varying noise levels.

2.2 Transfer Learning

The insufficiency of data sets is a prevalent issue faced by deep learning networks. Due to the sensitive nature of medical ultrasound images with respect to patient privacy, a similar lack of data sets is prevalent in this domain. Furthermore, even if abundant data sets were available, training a neural network from scratch would incur prohibitive costs. Consequently, most models aim to simplify the network to reduce data requirements. As a viable alternative, transfer learning can overcome these challenges effectively. In this paper, we adopt the definition of transfer learning by most researchers [12], which involves transferring pre-trained model parameters to enable new model training. Since most data or tasks are related in some way, transfer learning allows us to share the previously acquired model parameters with the new model, thereby accelerating and optimizing learning efficiency without the need to start from scratch [13].

3 Proposed Method

3.1 Plane-wave Imaging Technique

In the clinical setting, acquiring a sizeable corpus of clear ultrasound images alongside noisy counterparts proves arduous. In addition, it is imperative to preserve the unaltered fine structure of the denoised image owing to the unique attributes of medical images. To tackle this predicament, we leverage the plane-wave imaging technique to simulate a vast number of noisy ultrasound images that align with clean natural images, thus constituting the training dataset. Plane-wave imaging improves imaging frame rates significantly by concurrently activating the entire aperture of the array, thereby generating images of the complete region in a single emission [14, 15].To enhance the quality of plane-wave imaging, coherent plane wave compounding (CPWC) was proposed [16]. A uniform linear transducer array comprising N elements is used for transmission and reception. The received delayed echo signals from the aperture are delay-compensated based on their distances from the imaging point $P(x_p, z_p)$. The delay-compensated signals are then coherently summed to create the output of a single plane wave imaging (PWI) as expressed by Eqn. (1):

$$Y_{PWI}(p) = \sum_{i=0}^{N-1} \omega_i \, x_i(p) \qquad (1)$$

where ω is the weighting factor of length N, and $x_i(p)$ is defined as a vector containing the RF data recorded by the i-th element, corresponding to each pixel $P(x_p, z_p)$ in the imaging field. Assuming that the transmit beam is steered in M different angles θ_m, then the final output of CPWC imaging can be obtained by coherently summing the values obtained from each plane wave for the imaging point $P(x_p, z_p)$, and can be defined as Eqn. (2):

$$Y_{CPWCI}(p) = \frac{1}{M} \sum_{m=1}^{M} Y(p, \theta_m) \qquad (2)$$

The collected backscattered ultrasound signal $x_i(p)$ in Eqn. 1 can be expressed as the convolution of the tissue reflectivity function (TRF) and the point spread function (PSF) of the imaging system. The TRF represents the pixel information of the pristine natural image, it accounts for the position and size of the pixels and replaces the position and scattering intensity of the scatterers, respectively. Nevertheless, due to various assumptions of the ultrasound imaging system, the observed signal $x_i(p)$ can only signify an approximation of the real signal, more specifically, the collected ultrasonic signal consists the original signal as well as various noise and interference items, in which case the signal model in Eqn. (1) can be modified into:

$$x_i(p) = o_i(p) m_i(p) + a_i(p) \qquad (3)$$

where $m_i(p)$ and $a_i(p)$ represent the components of the multiplicative and additive noise respectively, and $o_i(p)$ and $x_i(p)$, the original and observed signal respectively.

Consequently, the evaluated ultrasound noise level can be expressed as the difference between the acquired signal and the real signal, it can be expressed by the Eqn.4:

$$N(p) = Y(p) - O(p) \qquad (4)$$

where N(x,y), Y(x,y), and O(x,y) indicate the noisy image, the transferred ultrasound image, and the natural image, respectively.

3.2 Denoiser Analysis

We use FFDNet as our basic network which utilizes a flexible and efficient network architecture for image denoising. It can handle varying noise levels and spatially transformed noise by taking a controllable noise level map as input. The input clean image (IM_i) has a size of $c \times h \times w$. To improve processing speed, IM_i is sliced into $c \times h/2 \times w/2$ patches using a downsampling technique. The patches are grouped into different channels based on their colors, resulting in a total of 4 channels, each with a size of $c \times h/2 \times w/2$. Consequently, the image pixels become 1/4 of their original size. In FFDNet, Additive White Gaussian Noise (AWGN) is used to emulate camera noise. AWGN follows the Gaussian distribution and is added to IM_i to produce a noisy image ($NM_{i)}$).

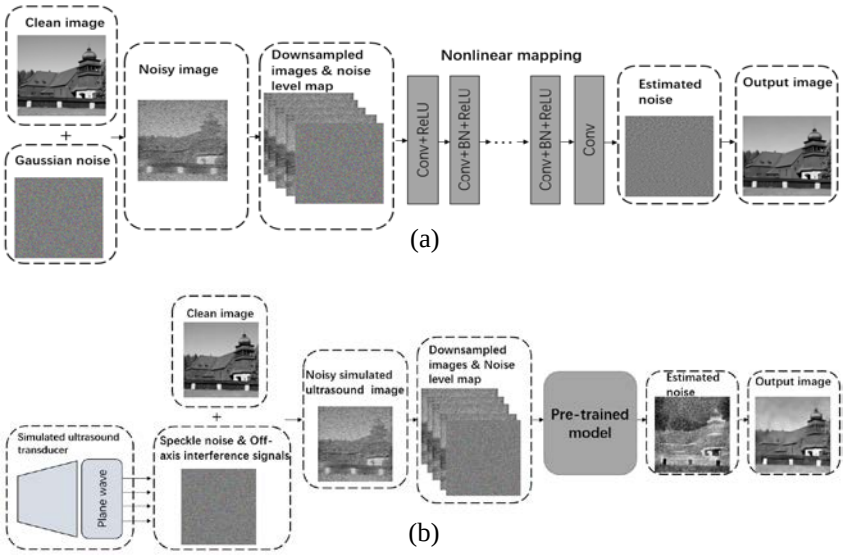

Fig. 1. (a) Architecture of Pre-trained Model for Noisy Natural Image Denoising, (b) Architecture of Deep Learning with Noise Transfer Learning for Simulated Noisy Ultrasound Image Denoising.

The different AWGN are generated according to different noise levels (σ) and combined with the four downsampled submaps to form a five-channel noisy image. The first layer comprises Conv+Relu, The intermediate layer assumes a convolution form, employing multiple Conv+BN+Relu operations. BN has the ability to enhance the convergence of the neural network model and improve the generalization of the

model. The ultimate layer is Conv, which executes convolution using a filter of size n × f × f. The loss is determined as Eqn. (5),

$$\mathrm{L}(\theta) = \frac{1}{2m}\sum_{i=1}^{\mathrm{m}} \left\| \mathrm{F}\left(NM_{i,}\sigma;\theta\right) - \mathrm{IM_i} \right\|^2 \qquad (5)$$

Adam is a first-order optimization algorithm that facilitates iterative updates to the weight of a neural network by utilizing training data. Specifically, when Adam is utilized to compute the minimum value of the loss, the loss gradually decreases during the training process at different epochs.

3.3 Noise Transfer Learning Model

Transfer learning entails transferring the trained parameters of a pre-existing model to aid in the training of a new model [17]. The pre-trained and newly trained models are affiliated in terms of the majority of the data or tasks. Specifically, the pre-trained model is trained using natural images that include additive noise, whereas the transfer learning model is trained using ultrasound images that encompass speckle noise, and other forms of clutter noise. The transfer learning technique utilized in this paper gradually progresses from simple additive noise denoising to complicated noise denoising present in ultrasound images. We have designated natural images in the pre-trained model as the domain source (DS), and the task of denoising natural images as the learn source (LS). Transfer learning involves using simulated noisy ultrasound images as domain target (DT), and learning target (LT) involves the denoising of ultrasound images. The goal of transfer learning is to enhance object inference in DT, drawing on knowledge learned in DS and LS. Specifically, transfer learning capitalizes on similarities between the features of DS and DT, as both focus on image learning. DS incorporates natural images with additive white Gaussian noise (AWGN), while DT involves simulated noisy ultrasound images with speckle noise, among other variations. The pre-trained model as shown in Fig. 1(a).The loss of the noise transfer learning model differs from the pre-trained model.

$$L(\theta) = \frac{1}{2\mathrm{m}}\sum_{\mathrm{i}=1}^{\mathrm{m}} \|\mathrm{F}(NM_i;\theta) - \mathrm{IM_i}\|^2 \qquad (6)$$

The loss, denoted by L(θ), is computed based on both real and estimated noise as shown in Eqn. (6). Where IM_i is clean image，NM_i is simulated noisy ultrasound image, θ is noise level map.

3.4 Downsampled Images

In this study, for improvimg the execution efficiency of the model, we leveage a reversible down-sampling layer that shapes the input image into a series of smaller sub-images. Specifically, we set the down-sampling factor to 2, which substantially enhances speed without reducing modeling ability. The down-sampled sub-image is presented to the CNN for feature extraction, which consequently extends the receptive field. Finally, the image is restored by upsampling.

3.5 Noise Level Map and Model without Noise Transfer Learning

To enable flexible adjustment of image denoising intensity, a noise level map can be employed to regulate the denoising level of the denoiser. In [18], the technique of adjusting the noise level map is applied to add noise to the image, which bears resemblance to the approach presented in this study. Figs.1 demonstrate the integration of the noise level map with the input image in a Convolutional Neural Network (CNN). The input image is segmented into patches, and the obtained noise level map is joined with the input image to create a new channel. In Fig. 1(a), σ represents the noise level, which is randomly selected from a uniform distribution. Different from the pre-trained model, in Fig. 1(b) actual noise is measured initially. The standard deviation (STD) of the noise is estimated using Eqn. (7).

$$\sigma = \sqrt{\frac{\sum_{i=1}^{n}(x_i - \bar{x})^2}{n-1}} \qquad (7)$$

σ represents the noise level of an ultrasound image, where $\bar{x}$ denotes the image's average noise level and x_i represents the pixel value of the noisy image. As STD is a real number and cannot be applied to a batch of images, we formulate a batchsize noise level map by combining the noise across the batch of images. The degree of denoising and preservation of image details varies with different noise level map. A high σ value indicates a greater degree of denoising, but a lower retention of image details.

This paper proposes denoisers for transfer learning and non-transfer learning that incorporate controllable noise level maps to accommodate different noise levels in denoising images, thereby enhancing the flexibility of our denoising model. In Eqn. (6), using noise=NM_i-IM_i, we can obtain the noise of each image in the training set, and then use Eqn. (7), we obtain the STD of noise, use Eqn. (6) to construct a loss, which can make our model flexible and controllable for non-blind denoising.For model without noise transfer learning, we use data set C to train CNN, σ value and loss in the same way as model with noise transfer learning.

4 Experimental Results

- **Dataset A**: The Waterloo Exploration Dataset (WED) [19] includes rich natural image information such as houses, cars, people, fruits, animals, etc. In order to facilitate the generation of simulated noisy ultrasound images and train model, we convert 4744 RGB natural images into gray.
- **Dataset B**: The Berkeley Segmentation Dataset (BSD400) [20] as validation dataset, it contains 400 grayscale images of size 180×180.
- **Dataset C**: 300 clean images which sourced from the WED and their corresponding simulated noisy ultrasound images as training dataset.
- **Dataset D**: The Berkeley Segmentation Dataset (BSD68) [21] as validation dataset, it contains 400 grayscale images of size 256×256.
- **Dataset E**: 50 breast ultrasound images for testing, obtained from the cooperative hospital .

Table 1. Datasets in this paper.

Dataset A	Dataset B	Dataset C	Dataset D	Dataset E
WED	BSD400	WED	BSD68	Breast ultrasound images
4744 images	400 images	300 images	68 images	50 images
RGB to gray	gray	RGB to gray	gray	gray
Not-fixed	180×180(size)	Not-fixed	256×256(size)	Not-fixed

4.1 Obtaining Simulated Noisy Ultrasound Image

The natural images datasets A, B, C, and D are transferred to the ultrasound image domain using the Field II simulator [22, 23]. The datasets are simulated using a standard L11-4v probe (Verasonics Inc., Redmond, WA). The probe settings as shown in Table 2, and the dataset used for model training was simulated using a 5.208 MHz transmission with a bandwidth of 77% and a sampling frequency of 30.4 MHz. Use dataset A, B, C, and D create 2-D distribution of scatterers whose depth is 10 cm based on the pixel information of the original image.

Table 2. Full parameters used in Field II simulator.

Parameter	Value	Parameter	Value
Center frequency f_c	7.6 MHz	Sampling frequency f_s	4 f_c
Element width	0.27 mm	Element kerf	0.03 mm
Number of elements	128	Pitch	0.3
Fractional bandwidth	77 %	Element height	5 mm
Speed of sound c	1540 m/s	Focal depth	18mm

4.2 Experiments on Pre-trained Model and Transfer Learning Model

The pre-trained model needs to be obtained by training it on Dataset A and validating it on Dataset B. As per the assumptions made in references [24], the noise in the camera can be considered as AWGN. To avoid introducing visual artifacts caused by the tradeoff between noise reduction, noise level adjustment, and image detail preservation, we employ the orthogonal initialization method for convolution filters. The results in Fig. 2(c) demonstrate that the pre-trained model yields superior denoising efficacy in natural image AWGN at different change spaces. Specifically, Fig. 2(f) indicates that the pre-trained model's denoising efficacy for ultrasound images is general. Therefore, further noise transfer learning is necessary to enhance the pre-trained model's capacity for denoising ultrasound images. The subsequent procedure involves an experiment in noise transfer learning.

The simulated noisy ultrasound images corresponding to Dataset c are fed into the pre-training model to continue training and then fine-tune the model parameters. To

achieve non-blind denoising and enhance the denoising performance for images with varying noise levels using the noise transfer learning model, we initially calculated the standard deviation of the noise to determine the noise level. Based on this, we constructed a noise level map containing the noise levels for a batch of images. The model was trained using simulated noisy ultrasound images and their corresponding noise level maps. Fig. 2(h) shows that our noise transfer learning model achieved state-of-the-art performance in denoising ultrasound images, and exhibited strong ability in denoising images with varying noise levels.

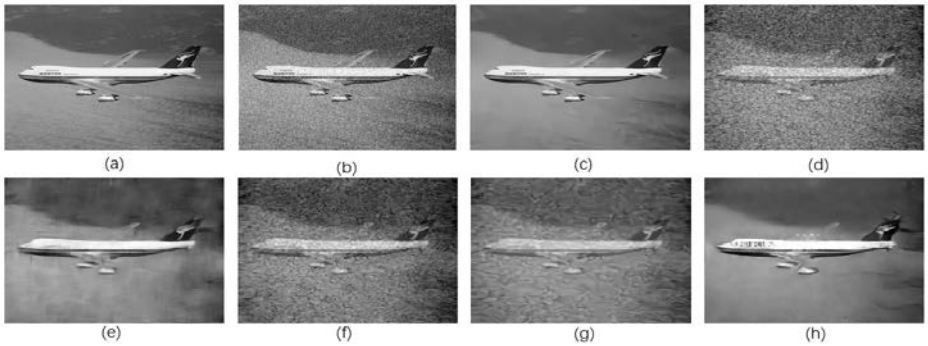

Fig. 2. Result of image denoising using different model . For natural image: (a) clean natural image, (b) AWGN noisy image, (c) denoising with Pre-trained Model. For simulated noisy ultrasound image: (d) simulated noisy ultrasound image, (e) denoising with CGAN, (f) denoising with Pre-trained Model, (g)denoising without transfer learning model, (h) denoising with transfer learning model. Denoising with transfer learning model achieves state-of-the-art.

Table 3. The results of PSNR、SSIM obtained from the other model for denoising simulated noisy ultrasound images. pix2pixGAN denoising does not need Sigma adjustment.

Model	**Sigma=25**		**Sigma=40**		**Sigma=55**	
	PSNR (dB)	**SSIM**	**PSNR (dB)**	**SSIM**	**PSNR (dB)**	**SSIM**
pix2pixGAN	23.51	0.7352	\	\	\	\
CNN Pre-trained model	21.93	0.7230	21.21	0.7115	19.61.	0.6236

4.3 Experiments Without Transfer Learning and Other Model

We use the CNN model for image denoising is discussed in Section 3.2 which is non-transfer learning, then we use Dataset D for testing. Results as shown in Table 3., the PSNR and SSIM performance are not as impressive as those with noise transfer learning method, and as Fig. 2(g) illustrates, the model without transfer learning is less effective than the noise transfer learning model.Then, the experiment is compared with other denoising methods. In recent years, there are serveral studies on image denoising using pix2pix Generative Adversarial Network (pix2pixGAN) [25, 26]. For the pix2pixGAN, we take the simulated ultrasound image as the input image and the clean image as the limiting condition, the denoised image was compared with the

clean image, leading a PSNR of 23.51 and SSIM of 0.7352, as shown in Table 3. The denoised image had distortion and contour distortion, as shown in Figure 2(e) .

4.4 Ablation Study

To justify the effectiveness of the model with transfer learning，we conducted the following experiments on Dataset D for testing. The detailed process of the experiment is described in section 4.2 and 4.3. See Table 4, when the noise level (our denoising parameter) was 40, model with transfer learning can enhance the average PSNR by approximately 3.17% and the average SSIM by approximately 10.84%. When the noise level was 25, model with transfer learning can enhance the average PSNR by approximately 6.99% and the average SSIM by approximately 9.40%. Obviously, the denoising effect of the model with transfer learning has been improved. When Sigma is greater than 25, the denoised image is too smooth, causing serious problems of blurred edges and loss of detail, so when Sigma is 25, the proposed model can achieve the best denoising effect.

Table 4. The results of PSNR、SSIM obtained from the proposed model with and without transfer learning for denoising simulated noisy ultrasound images.

Model	**Sigma=25**		**Sigma=40**		**Sigma=55**	
	PSNR (dB)	**SSIM**	**PSNR (dB)**	**SSIM**	**PSNR (dB)**	**SSIM**
Proposed model without transfer learning	23.15	0.8232	23.01	0.8035	20.15	0.6010
Proposed model with transfer learning	**24.77**	**0.9006**	**23.74**	**0.8906**	**20.88**	**0.6565**

4.5 Experiments on Real Ultrasound Images

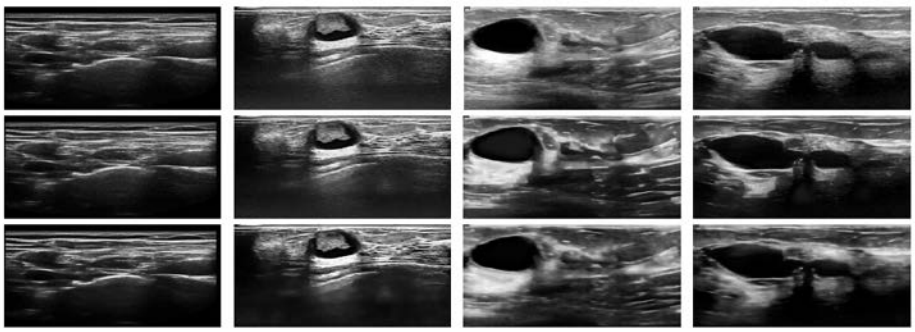

Fig. 3. From top to bottom: real breast ultrasound image, denoised image without transfer learning, denoised image with transfer learning.

Using dataset E, we fed real breast ultrasound images into pix2pixGAN and our noise transfer learning models. The denoising time of pix2pixGAN is 0.1572s, the time of

our proposed model is 0.1090s, and the denoising time is reduced by 44%, As shown in Fig. 3, we found that non-transfer learning will distort the ultrasound image and cause the loss of the details of the ultrasound image when the same noise level is employed. It is evident that the implementation of transfer learning for ultrasound image denoising purposes is substantially more effective than non-transfer learning.

5 Conclusion

This paper proposes a novel approach to denoise ultrasound images using a deep learning model, which incorporates a noise generation synthetic for fast and lightweight denoising. The model design and training involve the utilization of plane-wave imaging technique, CNN, transfer learning. However, using our proposed method to denoise the real ultrasound image, a small amount of speckle noise is still retained in the lesion area, and there is a slight distortion in the image. In the future, we will use the downstream task to verify the benefits from denoising, and invite clinicians to score images by observation, to verify the impact of the ultrasound image denoising model on clinical diagnosis.

Acknowledgment

This work was supported by Research Fund of Macao Polytechnic University (RP/FCA-05/2022), and Science and Technology Development Fund of Macao (0105/2022/A).

References

1. Quien, M.: Saric, M.: Ultrasound imaging artifacts: How to recognize them and how to avoid them[J]. Echocardiography35(9): 1388-1401(2018).
2. J. Dainty.: Some statistical properties of random speckle patterns in coherent and partially coherent illumination, Optica Acta, Int. J. Opt. vol. 17, no. 10, pp. 761–772(1970).
3. Sudha, S., Suresh, G.R., Sukanesh R.: Speckle noise reduction in ultrasound images by wavelet thresholding based on weighted variance[J]. International journal of computer theory and engineering 1(1): 7(2009).
4. C. A. Duarte-Salazar, A. E. Castro-Ospina, M. A. Becerra and E. Delgado-Trejos.: Speckle Noise Reduction in Ultrasound Images for Improving the Metrological Evaluation of Biomedical Applications: An Overview, in IEEE Access vol. 8, pp. 15983-15999(2020).
5. Mufeng Geng, Xiangxi Meng, Jiangyuan Yu, Lei Zhu, Lujia Jin, Zhe Jiang.: Content-Noise Complementary Learning for Medical Image Denoising, IEEE Transactions on Medical Imaging, vol. 41, no. 2, pp. 407-419(2022).
6. Goudarzi, S., Rivaz, H.: Deep reconstruction of high-quality ultrasound images from raw plane-wave data: A simulation and in vivo study[J]. Ultrasonics, 2022, 125: 106778.
7. Dabov, K., Foi, A., Katkovnik, V., & Egiazarian, K.: Image denoising by sparse 3-D transform-domain collaborative filtering. IEEE Transactions on image processing 16(8), 2080-2095 (2007).

8. Shuhang Gu, Lei Zhang, Wangmeng Zuo, and Xiangchu Feng. Weighted nuclear norm minimization with application to image denoising. In IEEE Conference on Computer Vision and Pattern Recognition (CVPR) 2862–2869, 1, 7, 8(2014).
9. Sil, Dibakar, Arindam Dutta, and Aniruddha Chandra. Convolutional neural networks for noise classification and denoising of images. TENCON 2019 IEEE Region 10 Conference (TENCON), IEEE(2019).
10. Zhang, K., Zuo, W., Chen, Y., Meng, D., & Zhang, L.： Beyond a gaussian denoiser: Residual learning of deep cnn for image denoising. IEEE transactions on image processing 26(7), 3142-3155 (2017).
11. K Zhang, W Zuo, L Zhang.： FFDNet: Toward a fast and flexible solution for CNN-based image denoising, IEEE Transactions on Image Processing, ieeexplore.ieee.org（2018).
12. Ribani, R., Marengoni, M.: A survey of transfer learning for convolutional neural networks. In 2019 32nd SIBGRAPI conference on graphics, patterns and images tutorials (SIBGRAPI-T) (pp. 47-57), IEEE(2019).
13. Mishkin, D., Matas, J.: All you need is a good init. arXiv preprint:1511.06422(2015).
14. O. Couture, M. Fink, M. Tanter.: Ultrasound contrast plane wave imaging, IEEE Trans. Ultrason., Ferroelectr., Freq. Control, vol. 59, no. 12, pp. 2676–2683(2012).
15. M. Tanter, M. Fink,: Ultrafast imaging in biomedical ultrasound, IEEE Trans. Ultrason., Ferroelectr., Freq. Control, vol. 61, no. 1, pp. 102–119(2014).
16. G. Montaldo, M. Tanter, J. Bercoff, N. Benech, M. Fink.: Coherent plane-wave compounding for very high frame rate ultrasonography and transient elastography, IEEE Trans. Ultrason., Ferroelectr., Freq. Control, vol. 56, no. 3, pp. 489–506(2009).
17. S. J. Pan, Q. Yang.: A Survey on Transfer Learning, in IEEE Transactions on Knowledge and Data Engineering, vol. 22, no. 10, pp. 1345-1359(2010).
18. Yao, H., Wang, S., Zhang, X., Qin, C., Wang, J.: Detecting image splicing based on noise level inconsistency. Multimedia Tools and Applications, 76, 12457-12479(2017).
19. Ma, K., Duanmu, Z., Wu, Q., Wang, Z., Yong, H., Li, H., & Zhang, L.: Waterloo exploration database: New challenges for image quality assessment models. IEEE Transactions on Image Processing 26(2), 1004-1016 (2016).
20. Martin, D:, Fowlkes, C., Tal, D., Malik, J.: A database of human segmented natural images and its application to evaluating segmentation algorithms and measuring ecological statistics. International Conference on Computer Vision 41:6_423(2001).
21. Roth, S., Black, MJ.: Fields of experts. International Journal of Computer Vision 82(2):205_229 DOI 10.1007/s11263-008-0197-6（2009).
22. J.A. Jensen, N.B. Svendsen.: Calculation of pressure fields from arbitrarily shaped, apodized, and excited ultrasound transducers, IEEE Trans. Ultrason. Ferroelectr. Freq. Control 39 (2) , 262–267(1992).
23. J.A. Jensen.: FIELD: A program for simulating ultrasound systems, in: 10th Nordic-Baltic Conference on Biomedical Imaging, Vol. 4, pp. 351–353(1996).
24. F. Luisier, T. Blu, M. Unser.: Image Denoising in Mixed Poisson–Gaussian Noise, in IEEE Transactions on Image Processing, vol. 20, no. 3, pp. 696-708(2011).
25. Isola, P., Zhu, J. Y., Zhou, T.: Image-to-Image Translation with Conditional Adversarial Networks[J]. IEEE(2016).
26. Alsaiari, A., Rustagi, R., Alhakamy, A., Thomas, M. M., Forbes, A. G.: Image Denoising Using A Generative Adversarial Network. IEEE 2nd International Conference on Information and Computer Technologies (ICICT), 126–132 (2019).